

Optimization of multi-cycle two-color laser fields for the generation of an isolated attosecond pulse

Byunghoon Kim,¹ Jungkwen Ahn,¹ Yongli Yu,² Ya Cheng,² Zhizhan Xu,²
and Dong Eon Kim,^{1,*}

¹Department of physics, Pohang University of Science and Technology(POSTECH), Pohang 790-784, Korea

²State Key Laboratory of High Field Laser Physics, Shanghai Institute of Optics and Fine Mechanics,
Chinese Academy of Sciences P.O. Box 800-211, Shanghai 201800, China

*Corresponding author: kimd@postech.ac.kr

Abstract: The effect of the mixing of pulsed two color fields on the generation of an isolated attosecond pulse has been systematically investigated. One main color is 800 nm and the other color (or secondary color) is varied from 1.2 to 2.4 μm . This work shows that the continuum length behaves in a similar way to the behavior of the difference in the square of the amplitude of the strongest and next strongest cycle. As the mixing ratio is increased, the optimal wavelength for the extended continuum shifts toward shorter wavelength side. There is a certain mixing ratio of intensities at which the continuum length bifurcates, i.e., the existence of two optimal wavelengths. As the mixing ratio is further increased, each branch bifurcates again into two sub-branches. This 2D map analysis of the mixing ratio and the wavelength of the secondary field easily allows one to select a proper wavelength and the mixing ratio for a given pulse duration of the primary field. The study shows that an isolated sub-100 attosecond pulse can be generated mixing an 11 fs full-width-half-maximum (FWHM), 800 laser pulse with an 1840 nm FWHM pulse. Furthermore the result reveals that a 33 fs FWHM, 800 nm pulse can produce an isolated pulse below 200 as, when properly mixed.

©2008 Optical Society of America

OCIS codes: (190.2620) Frequency conversion; (190.4160) Multiharmonic generation; (320.0320) Ultrafast optics.

References and links

1. K. Lee, Y. H. Cha, M. S. Shin, B. H. Kim, and D. Kim, "Relativistic nonlinear Thomson scattering as attosecond x-ray source," *Phys. Rev. E*, **3**, 67 026502 (2003).
2. J. Gao, "Thomson Scattering from Ultrashort and Ultraintense Laser Pulses," *Phys. Rev. Lett.* **93**, 243001 (2004).
3. K. Lee, Y. H. Cha, M. S. Shin, B. H. Kim, and D. Kim, "Temporal and spatial characterization of harmonic structures of relativistic nonlinear Thomson scattering," *Opt. Express* **11**, 309-316 (2003), <http://www.opticsinfobase.org/abstract.cfm?URI=oe-11-4-309>.
4. A. A. Zholents and G. Penn, "Obtaining attosecond x-ray pulses using a self-amplified spontaneous emission free electron laser," *Phys. Rev. STAB*, **8**, 050704 (2005).
5. P. Emma, K. Bane, M. Cornacchia, Z. Huang, H. Schlarb, G. Stupakov, and D. Walz, "Femtosecond and Subfemtosecond X-Ray Pulses from a Self-Amplified Spontaneous-Emission-Based Free-Electron Laser," *Phys. Rev. Lett.* **92**, 074801 (2004).
6. P. B. Corkum, N. H. Burnett, and M. Y. Ivanov, "Subfemtosecond pulses," *Opt. Lett.* **19**, 1870-1872 (1994).
7. G. D. Tsakiris, K. Eidmann, J. Meyer-ter-Vehn, and F. Krausz, "Route to intense single attosecond pulses," *New J. Phys.* **9**, 019 (2006).
8. K. Lee, B. H. Kim, and D. Kim, "Coherent radiation of relativistic nonlinear Thomson scattering," *Phys. Plasmas* **12**, 043107 (2005).
9. B. Dromey et al, "Bright Multi-keV Harmonic Generation from Relativistically Oscillating Plasma Surfaces," *Phys. Rev. Lett.* **99**, 085001 (2007)
10. M. Hentschel, R. Kienberger, Ch. Spielmann, G. A. Reider, N. Milosevic, T. Brabec, P. Corkum, U. Heinzmann, M. Drescher, and F. Krausz, "Attosecond metrology," *Nature* **414**, 509-513 (2001).

11. P. Tzallas, D. Charalambidis, N. A. Papadogiannis, K. Witte, and G. D. Tsakiris, "Direct observation of attosecond light bunching," *Nature* **426**, 267-271 (2003).
12. M. Drescher, M. Hentschel, R. Kienberger, G. Tempea, C. Spielmann, G. A. Reider, P. B. Corkum, and K. Krausz, "X-ray pulses Approaching the Attosecond Frontier," *Science* **291**, 1923-1927 (2001).
13. M. Paul, E. S. Toma, P. Breger, G. Mullot, F. Auge, Ph. Balcou, H. G. Muller, and P. Agostini, "Observation of a Train of Attosecond Pulses from High Harmonic Generation," *Science* **292**, 1689-1692 (2001).
14. Y. Mairesse, A. de Bohan, L. J. Frasinski, H. Merdji, L. C. Dinu, P. Monchicourt, P. Breger, M. Kovačev, R. Taieb, B. Carré, H. G. Muller, P. Agostini, and P. Salières, "Attosecond synchronization of high-harmonic soft X-rays," *Science* **302**, 1540-1543 (2003).
15. M. Schultze, E. Goulielmarkis, M. Uiberacker, M. Hofstetter, J. Kim, D. Kim, F. Krausz, and U. Kleineberg, "Powerful 170-attosecond XUV pulses generated with few-cycle laser pulses and broadband multilayer optics," *New J. Phys.* **9**, 243 (2007).
16. Z. Zeng, Y. Cheng, X. Song, R. Li, and Z. Xu, "Generation of an Extreme Ultraviolet Supercontinuum in a Two-color Laser Field," *Phys. Rev. Lett.* **98**, 203901 (2007).
17. X. Song, Z. Zeng, Y. Fu, B. Cai, R. Li, Y. Cheng, and Z. Xu, "Quantum path control in few-optical-cycle regime," *Phys. Rev. A.* **76**, 043830 (2007).
18. T. Pfeifer, L. Gallmann, M. J. Abel, P. M. Nagel, D. M. Neumark, and S. R. Leone, "Heterodyne Mixing of Laser Fields For Temporal Gating of High-order Harmonic Generation," *Phys. Rev. Lett.* **97**, 163901 (2006).
19. Y. Huo, Z. Zeng, R. Li, and Z. Xu, "Single attosecond pulse generation using two-color polarized time-gating technique," *Opt. Express* **13**, 9897-9902 (2005), <http://www.opticsexpress.org/abstract.cfm?URI=OPEX-13-24-9897>.
20. M. Kovačev, Y. Mairesse, E. Priori, H. Merdji, O. Tcherbakoff, P. Monchicourt, P. Breger, E. Mével, E. Constant, P. Salières, B. Carré, and P. Agostini, "Temporal con-finement of the harmonic emission polarization gating," *Eur. Phys. J. D* **26**, 79-82 (2003).
21. C. Altucci, Ch. Delfin, L. Roos, M. B. Gaarde, A. L'Huillier, I. Mercer, T. Starcze-wski, and C.-G. Wahlström, "Frequency-resolved time-gated high-order harmonics," *Phys. Rev. A* **58**, 3941-3934 (1998).
22. Y. Yu, X. Song, Y. Fu, R. Li, Y. Cheng, and Z. Xu, "Theoretical investigation of single attosecond pulse generation in an orthogonally polarized two-color laser field," *Opt. Express* **16**, 686-694 (2008), <http://www.opticsinfobase.org/abstract.cfm?URI=oe-16-2-686>.
23. G. Sansone, et al "Isolated single-cycle attosecond pulses," *Science* **314**, 443-446 (2006).
24. H. Merdji, T. Auguste, W. Boutu, J.-Pascal Caumes, B. Carre, T. Pfeifer, A. Jullien, D. M. Neumark, and S. R. Leone, "Isolated attosecond pulses using a detuned second-harmonic field," *Opt. Lett.* **32**, 3134-3136 (2007), <http://www.opticsinfobase.org/abstract.cfm?URI=ol-32-21-3134>.
25. M. Lewenstein, Ph. Balcou, M. Y. Ivanov, A. L'Huillier, and P. B. Corkum, "Theory of high-harmonic generation by low-frequency laser fields," *Phys. Rev. A.* **49**, 2117-2132 (1994).
26. M. B. Gaarde and K. J. Schafer, "Space-Time Considerations in the Phase Locking of High Harmonics," *Phys. Rev. Lett.* **89**, 213901 (2002).
27. P. Antoine, A. L'Huillier, and M. Lewenstein, "Attosecond Pulse Trains Using High-Order Harmonics," *Phys. Rev. Lett.* **77**, 1234-1237 (1996).
28. C. Vozzi, F. Calegari, E. Benedetti, S. Gasilov, G. Sansone, G. Cerullo, M. Nisoli, S. De Silvestri, and S. Stagira, "Millijoule-level phase-stabilized few-optical-cycle infrared parametric source," *Opt. Lett.* **32**, 2957-2959 (2007), <http://www.opticsinfobase.org/abstract.cfm?URI=ol-32-20-2957>.

1. Introduction

The ultrafast phenomena which occur in shorter than 1 femtosecond time scale have not been explored much up to now. An attosecond pulse is an essential tool to investigate such ultrafast phenomena. To generate attosecond pulses, several methods such as relativistic nonlinear Thomson scattering (RNTS) [1-3], undulator radiation from energy-modulated electron beam [4,5], high order harmonics generation(HHG) from gas [6] and solid surface [7] have been suggested.

Because RNTS method requires a laser intensity of higher than $1 \times 10^{18} \text{ W/cm}^2$ and a sensitive coherent condition [8], the attosecond pulse generation by RNTS has not been demonstrated yet. Recently B. Dromey *et al.* reported the generation of X-rays of up to 3.5keV energy by using surface harmonic method [9]. X-ray pulse duration was not yet measured. To generate a clean isolated attosecond pulse, the laser intensity of larger than $1 \times 10^{18} \text{ W/cm}^2$ with a contrast ratio of 10^{10} is required.

The approach using HHG from gas has been successful to generate attosecond XUV pulse because of the required laser intensity being moderate and the simple experimental geometry [10-15]. Because the radiation is emitted by each half-cycle of a laser field in the HHG approach, an attosecond pulse train is naturally generated using a multi cycle laser. P. M. Paul *et al.* produced a train of 250 as xuv pulse using a 40 fs laser system [13]. A pulse train of 130 as was obtained by the synchronization of harmonics on attosecond time scale [14]. An isolated attosecond pulse is more useful in applications than an attosecond pulse train. For the generation of an isolated attosecond pulse, a large difference between the strongest and the next strongest electric field within the laser envelope is preferred. A few-cycle laser such as 5 fs full-width-half maximum (FWHM) laser has naturally this property. M. Schultze *et al.* reported the generation of 170 as isolated pulse using 5 fs FWHM laser pulses [15]. To get a even shorter isolated pulse by a larger electric field strength difference with few-cycle lasers or to get an isolated attosecond pulse by multi-cycle lasers whose electric field changes slowly within the laser envelope, the mixing of two color fields or polarizations have been proposed [16-22]. The mixture of different color and amplitude fields can result in a larger difference in the field amplitude among neighboring cycles than in a single color field. The mixing of 6 fs FWHM, 800 nm laser with 21.3 fs FWHM, 400 nm [16] or 64 fs FWHM, 2400 nm [17] has been theoretically studied, showing that a sub-100 as pulse can be generated. Recently an isolated 130 as pulse was experimentally demonstrated using polarization gating [23]. In all of these works, high harmonics or sub-harmonics of the fundamental field were used. No systematic work has been done for the effect of arbitrary wavelength being mixed. H. Merdji *et al.* showed that the mixing of detuned 2nd harmonic of a 800 nm, 40 fs FWHM pulse (the fundamental field) can generate sub-100 as pulse more efficiently than the mixing of the 2nd harmonic [24].

In this paper, we discuss the effect of mixing the two color fields on the generation of an isolated attosecond pulse and show that there exist optimal wavelengths for the generation of the shortest isolated attosecond pulse. In our study, an 800 nm laser field is mixed with another laser field from 1200 nm to 2400 nm wavelength region, which can be generated by optical parametric processes from an 800 nm laser field. Recently C. Vozzi *et al.* has demonstrated the phase stabilization of infrared few cycle pulse generated by optical parametric process up to mJ level [28]. A series of experiments for the simulation results presented in this work is viable.

2. Continuum analysis

HHG from gas (or atom) under a strong laser field is well described by the 3-step model [25]: a bound electron initially is first ionized via tunneling, and then it travels in the oscillating laser field until being driven back to its parent ion. Finally it recombines with the parent ion, emitting photons. The maximum photon energy that can be released is proportional to the ponderomotive energy that the electron has gained during travel under the laser field. Since the ponderomotive energy scales with the square of the laser field amplitude, the maximum photon energy is directly related to the laser intensity.

The tunnel ionization is very sensitive to laser intensity. A bound electron is likely to be ionized near the peak of the laser envelope where the amplitudes of optical cycles are large. The electron returns to its parent ion in the next optical cycle. Photons are emitted every nearly-half-cycle around the peak of the laser envelope as shown in Fig. 1(a). Figure 1(a) is the time-frequency diagram which shows when and what kind of the photons are generated. Note that there are 4 major emissions in Fig. 1(a). Each emission has the time structure that the low energy photons are emitted two times and the high energy photons are emitted one time. As seen in Fig. 1(a), the photons around 100eV are emitted 5 times (around +0.75 fs (strong), +0.4 fs, +0.2 fs (medium), -0.2 fs and -0.4 fs (weak)). Their time integrated spectrum is modulated as shown in Fig. 1(b). On the other hand, the photons around 140eV are emitted only one time (+0.15 fs) so that their spectrum is smooth. We call the smooth part of the spectrum as continuum. These photons consist of an isolated attosecond pulse. The larger the spectral width of this continuum is, the shorter the pulse width can be.

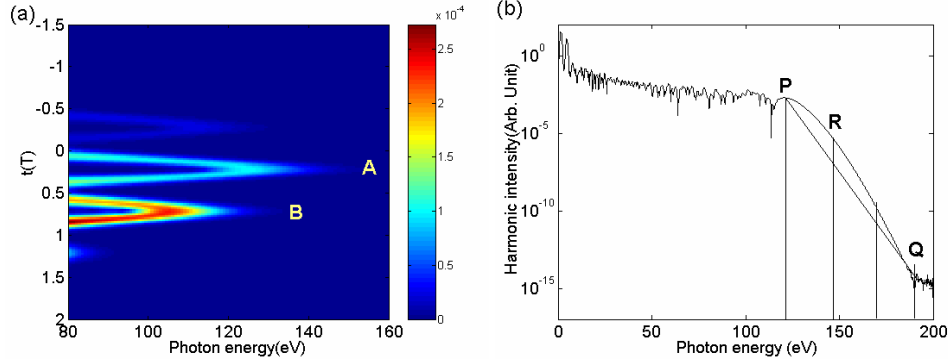


Fig. 1. (a) time-frequency diagram (b) its time-integrated spectrum (high harmonic spectrum)
The simulation was done for a 5fs FWHM, 800nm laser of $5 \times 10^{14} \text{ W/cm}^2$ interacting with He atom

The continuum length is the spectral width of this smooth part of the spectrum in the high energy side. We define the continuum length in this way: the start point of the continuum is the photon energy where its intensity emitted in the widest emission (say the emission A in Fig. 1(a)) is 3 times larger than its intensity in the 2nd widest emission (say the emission B in Fig. 1(a)). The end point is the first 1/3 point (R as shown in Fig. 1(b)) between the local maximum point (P) of the continuum and the start of noise (Q). The continuum length is then the difference between this start and end point. In the case of Fig. 1(b), the start point is 120 eV and the end point 145 eV so that the continuum length is 25 eV. In most of simulation cases in our current study, the photon intensity at the end point is about 1% of the photon intensity at P point. This determination of the end point is not absolute. Another way may be taken that the end point is the photon energy at which the extension of the plateau of high harmonic spectrum and the tangential line of the steepest slope to the falling edge meets. This way also results in a similar conclusion. The determination of the continuum length in the above way is the trade-off between the cleanness and the shortness of an isolated attosecond. If the continuum is taken too large, the contribution from other emissions contained is significant enough that the pulse shape has a complicated structure like that shown in Fig. 5(e). If the continuum is taken too short, the pulse duration is not as short as it can be.

This definition of the end point is similar to the way in which we find out the cut-off photon energy in each emission of A and B. The cut-off photon energy in each emission is proportional to the ponderomotive energy, which scales as the square of the laser electric field. Hence it is a good approximation that the continuum length is proportional to the difference between the square of the strong electric field and the 2nd strongest electric field, as well shown below in Figs. 3(a) and (b).

Using the Lewenstein model, we investigate systematically how the mixing of the two color fields affects the generation of continuum and show that there exist optimal wavelengths for the generation of the shortest isolated attosecond pulse.

In our study, an 800 nm light is primary because the 800 nm light is the center wavelength of most popular Ti:S fs lasers. An 800 nm laser field is mixed with another laser field from 1200nm to 2400nm wavelength region, which can be generated by optical parametric processes from an 800 nm laser field. We consider the mixing of linearly-polarized light. The electric field, when two color fields are mixed, can be written:

$$E = E_1 \exp(-2 \ln 2 \frac{t^2}{\tau_1^2}) \cos(\omega_1 t + \phi_1) + E_2 \exp(-2 \ln 2 \frac{t^2}{\tau_2^2}) \cos(\omega_2 t + \phi_2), \quad (1)$$

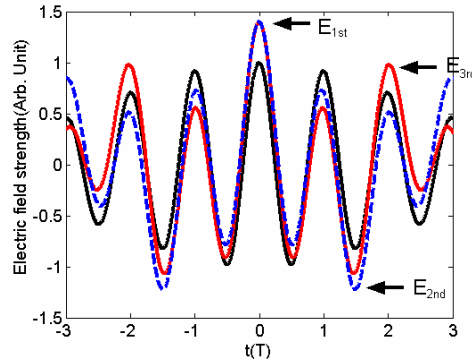


Fig. 2. The electric field of single and mixed laser field. The black line is the electric field of a linearly polarized 11fs FWHM, 800nm laser(single color), the red line the field of 11 fs FWHM, 800nm laser mixed with, 64fs FWHM, 1840nm laser of 16% intensity of 800 nm light, and the dotted blue line the field of 11 fs FWHM, 800nm laser mixed with 1200nm laser . E_{1st} means the strongest peak electric field. E_{2nd} E_{3rd} are second, third one. E_{1st} is overlapped at blue and red line. T is the period of 800 nm light

where E_1 and E_2 are the electric field amplitudes, ω_1 and ω_2 the frequencies, τ_1 and τ_2 the pulse width (FWHM), ϕ_1 and ϕ_2 the phases of the two color fields, Figure 2 shows how the electric field changes when two colors are mixed. The black line shows the field of 800 nm, 11 fs FWHM laser light (single color). The red line is the field when the 800 nm, 11 fs FWHM light field is mixed with an 1840 nm, 64 fs FWHM light pulse whose intensity is 16% of the 800 nm light. The dotted blue line is the case where a 1200nm, 64 fs FWHM light, with its intensity being 16% intensity of an 800 nm light is mixed with the 800 nm, 11 fs FWHM light. The phases are set to be zero. E_{1st} denotes the most strongest electric field, and E_{2nd} , E_{3rd} the second and third one, respectively. In the case of the blue line, the ratio E_1/E_{2nd} does not change much but E_1/E_{3rd} is improved. In the case of the red line, both E_1/E_{2nd} and E_1/E_{3rd} are improved. This shows that the field amplitude changes sensitively to a mixing condition. Because the maximum energy of harmonics is proportional to the square of the laser electric field, under which the free electron travels, the continuum length is approximately proportional to the difference in between E_{1st}^2 and E_{2nd}^2 . Since the transform-limited pulse duration of a light pulse is inversely proportional to its bandwidth, the continuum length should be increased for a shorter isolated attosecond pulse. To increase the continuum length, the peak intensity difference, $E_{1st}^2 - E_{2nd}^2$, should be enlarged. So we define an intensity difference ratio δ_d between the strongest and the 2nd strongest peak by

$$\delta_d = \frac{E_{1st}^2 - E_{2nd}^2}{E_{1st}^2} \quad (2)$$

The variation of the intensity difference ratio with respect to the mixing wavelength and its amount is shown in Fig. 3. The primary field is the 800 nm, 11fs FWHM laser field of $5 \times 10^{14} W/cm^2$. Figure 3(a) shows the variation (solid square) of δ_d with respect to the wavelength of the secondary field whose intensity is 4 % of the primary laser intensity. The continuum length (solid triangle), measured as described in the above, is also plotted. Note that both the intensity ratio and the continuum length change in a similar way. The change with respect to the mixing wavelength is dramatic: for the case of an 11fs FWHM 800nm single color (black line in Fig. 2) δ_d is 0.05. For the case of a 1200 nm light being mixed, δ_d

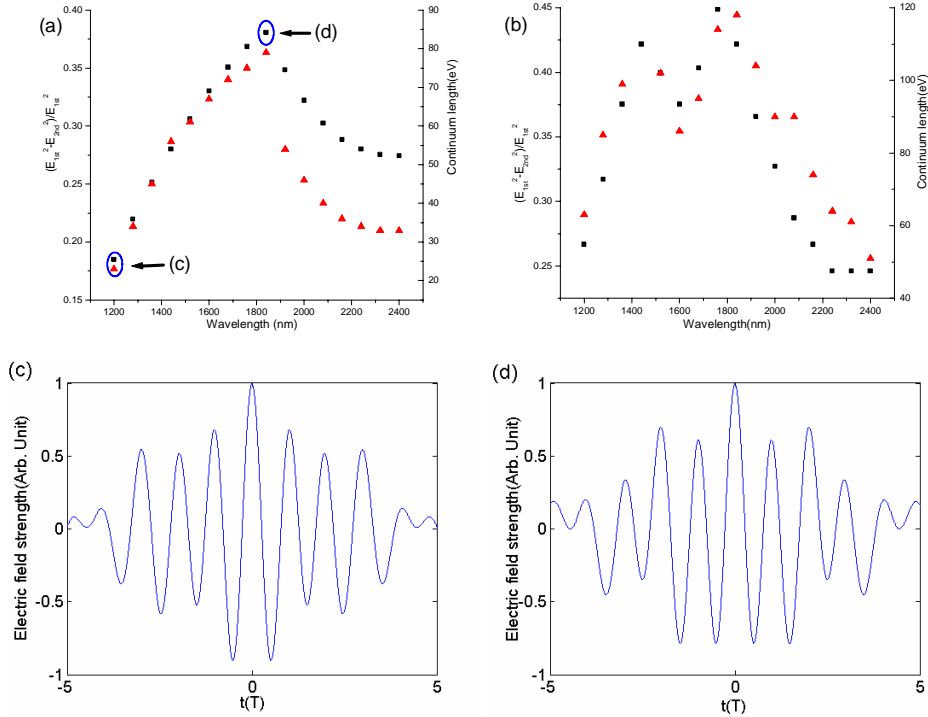


Fig. 3. Laser intensity difference (■) and continuum length (▲) in case of a linearly polarized 11fs FWHM laser pulse of $5 \times 10^{14} \text{ W/cm}^2$ mixed with a 64 fs FWHM secondary pulse of different intensities: (a) $2 \times 10^{13} \text{ W/cm}^2$ (4%) for Ar (b) $8 \times 10^{13} \text{ W/cm}^2$ (16%) for He. The horizontal axis is the wavelength of the secondary field. (c) The electric field of the condition as marked by (c) in (a). (d) The electric field of the condition as marked by (d) in (a).

is 0.18, and for the case of 1840nm being mixed, δ_d is 0.38 and the continuum length is almost doubled. This clearly demonstrates that the mixing of the secondary field with only a few % of the intensity of the primary field can dramatically change δ_d , which is directly related to the continuum length. When the intensity of the secondary field is increased to e.g. 16% of the primary field, it is observed as shown in Fig. 3(b) that both the intensity ratio and the continuum length have a double peak structure, indicating that there are two optimum wavelengths (1440 nm and 1840nm) for an extended continuum length. The examination of the electric field reveals that $E_{2nd} = E_{3rd}$ at the optimum wavelength [Fig. 3(d)]. Since the improvement in the intensity ratio comes from the beating between different wavelengths, the optimum wavelength is not necessarily the sub-harmonic of the primary field such as $\omega_2 = 1/2\omega_1$, $\omega_2 = 1/3\omega_1$, etc. Such sub-harmonics have a constructive interference at the second or third peak when mixed with their fundamental field, which is not favorable to the generation of a longer continuum length.

As can be noticed in Eq. (1), the intensity difference ratio is a function of wavelengths (ω_1 and ω_2), amplitude ratio (E_1 and E_2), phase (ϕ_1 and ϕ_2) and pulse durations (τ_1 and τ_2) of two color fields. We investigate how the intensity difference ratio (δ_d) depends on these parameters. Instead of a complete scan in 8 dimensional parameter space which demands tremendous effort, we limit ourselves to a parameter space, considering real experimental

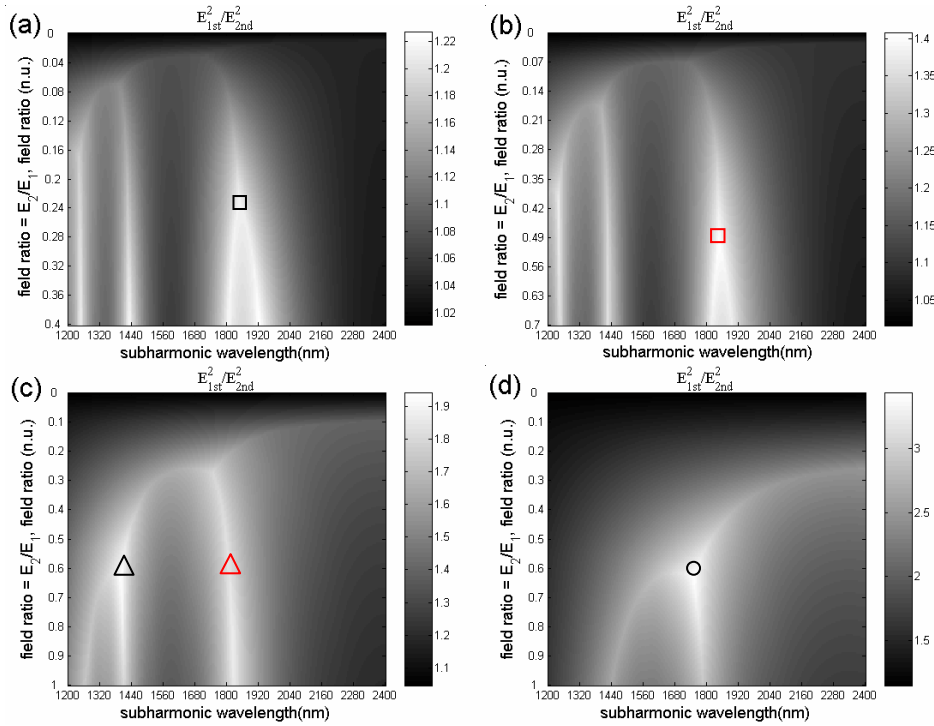


Fig. 4. Contour maps of intensity ratio, $(E_2/E_1)^2$, for various fundamental pulse durations with respect to the field ratio and the wavelength of the secondary field whose pulse duration is 64fs FWHM. The pulse duration(FWHM) of the primary field is 33 fs for (a), 22 fs for (b), 11 fs for (c), and 6 fs for (d).

Table 1. Thresholds for bifurcation

	Fundamental laser pulse duration			
	33 fs	22 fs	11 fs	6 fs
Threshold ratio (E_2/E_1)	0.03	0.07	0.28	0.62

conditions: the primary field is 800 nm light (ω_1 is the frequency of 800 nm light) with an intensity of $5 \times 10^{14} W/cm^2$, weaker than which the intensity of the secondary field is. The wavelength of the secondary field is chosen to be longer than the primary because the longer wavelength is in general more favorable to reduce the amplitude of the 2nd strongest cycle of the primary field. The pulse duration of the secondary field is chosen to be 64 fs FWHM. An infrared light of this duration with a reasonable energy (up to mJ level) is available for real experiments through optical parametric progresses even with phase stabilization [28].

Figure 4 is the 2-D contour map of $(E_2/E_1)^2$, showing the variation in δ_d with respect to the wavelength of the secondary field and amplitude ratio E_2/E_1 for different pulse durations of the primary field. The x-axis is the wavelength of the secondary field and the y-axis the amplitude ratio, E_2/E_1 .

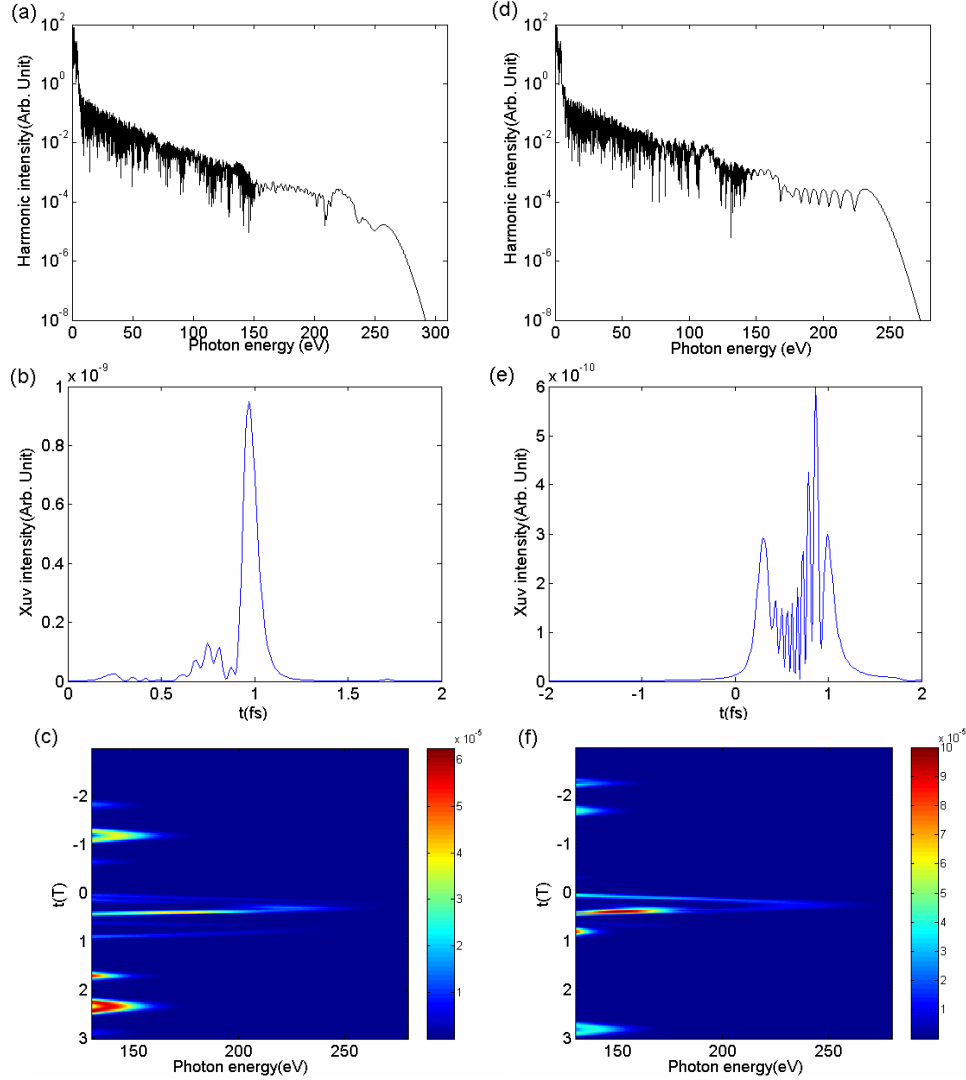


Fig. 5. High harmonic spectrum (a), generated isolated attosecond pulse (b) and time frequency diagram(c) for the mixing of an 11 fs FWHM, 800nm, and $3 \times 10^{14} W/cm^2$ with a 64 fs FWHM, 1840nm, $1.1 \times 10^{14} W/cm^2$. This is the condition for the red triangle in Fig. 4(c); (d), (e), and (f) for the mixing of an 11 fs FWHM, 800nm, and $3 \times 10^{14} W/cm^2$ with a 64 fs FWHM, 1400nm, and $1.1 \times 10^{14} W/cm^2$. This is the condition for the black triangle in Fig.4(c)

To bring up the minute change in δ_d more clearly, instead of δ_d , we plot the ratio $r_l = E_{1st}^2 / E_{2nd}^2 = 1 / (1 - \delta_d)$ in Fig. 4. While δ_d varies between 0 and 1, (since E_{1st} is bigger than E_{2nd}), r_l changes from unity to infinity ($1 < r_l < \infty$). When δ_d increases, r_l increases more rapidly so that r_l can show even a minute change in δ_d more clearly. The pulse durations (FWHM) of the primary field are different for Figs. 4(a)-(d): (a) 33 fs (b) 22 fs, (c) 11 fs, and (d) 6 fs. The bright color means a long continuum length (or shorter attosecond pulse in time domain) In Fig. 4(a), for a given $E_2 / E_1 = 0.36$, four bright colors exist, which means that there are four optimum wavelengths which can produce extended continua. Examining Figs. 4(a)-(d), note that as the amplitude ratio is increased, the bright color (or correspondingly, the

optimum wavelength for an extended continuum) shifts from longer wavelength (2400 nm) to shorter wavelength (1200 nm). At a certain wavelength, it bifurcates into two branches. Each branch bifurcates again at a different level of E_2/E_1 . Notice that the threshold amplitude ratio at which the bright color (or the optimum wavelength) bifurcates gets higher as the pulse duration of the primary field gets shorter. The threshold ratio is 0.03 and 0.62 in the case of 33 fs FWHM pulse (Fig. 4(a)) and 6 fs FWHM (Fig. 4(d)), respectively, as tabulated in Table 1.

This is rather easily understood that as the pulse duration gets shorter, the difference between the strongest and the next strongest amplitude gets bigger. Hence the mixing with larger amplitude of the secondary field is required.

3. Isolated attosecond pulse

The continuum analysis described in the section 2 allows one to find the optimum wavelength for a given condition. In each of Fig. 4, the specifications of the secondary laser field for extended continua were chosen (marked as square, circle, and triangle) and the corresponding attosecond pulse durations were found out. Helium was used as a working gas medium. A 90 attosecond isolated pulse is expected for the mixing of an 800 nm, 6 fs FWHM pulse of $3 \times 10^{14} \text{ W/cm}^2$ with an 1760 nm, 64 fs FWHM pulse of $1.1 \times 10^{14} \text{ W/cm}^2$ [circle in Fig. 4(d)] The continuum extends from 130 to 280 eV. The Fourier-transform limited pulse duration of this continuum length is 35 attoseconds. To achieve this, extra chirp management is required.

The mixing of an 800nm, 11 fs FWHM pulse of $3 \times 10^{14} \text{ W/cm}^2$ with an 1840 nm, 64 fs FWHM pulse of $1.1 \times 10^{14} \text{ W/cm}^2$ [red triangle in Fig. 4(c)] is expected to produce an isolated pulse of 80 attosecond, as shown in Fig. 5(b). Figures 5(a)-(c) are spectrum (a), time structure (b), and time frequency diagram (c) for the condition of the red triangle in Fig. 4(c). The continuum covers from 160 to 260 eV [Fig. 5(a)]. If one is able to select this continuum using XUV optics such as multilayer mirror and/or a filter, an isolated single 80 attosecond pulse is expected to be produced. With a careful chirp management this pulse can be shortened even down to 45 attosecond pulse.

As shown in the section 2, there is another optimum wavelength (1400 nm) when the mixing ratio is larger than the threshold in the case of an 11 fs FWHM, 800 nm laser. The condition for an extended continuum is 11 fs FWHM, 800nm $3 \times 10^{14} \text{ W/cm}^2$ and 64 fs FWHM, $1.1 \times 10^{14} \text{ W/cm}^2$ (black triangle in Fig. 4(c)). Figures 5(d)-(f) are spectrum (d), time structure (e), and time frequency diagram (f) for the condition of the black triangle in Fig. 4(c). Both cases have resulted in a similar intensity difference and continuum length (from 160 to 260 V). However, the expected pulse durations are quite different. This can be understood by examining the time-frequency diagram. In the continuum region of 160 to 260 eV, in the case of 1840 nm, the radiation by electrons in a long trajectory is much stronger than that by electrons on a short trajectory [Fig. 5(c)] so that a single pulse appears [Fig. 5(b)]; on the other hand, in the case of 1400nm, the radiations by both trajectories are equally strong [Fig. 5(f)], resulting in a complicated pulse [Fig. 5(e)]. It has been experimentally shown that the contribution of long trajectory radiation can be minimized with a suitable harmonic generation condition [26, 27]. Therefore the 1400nm case may still generate attosecond pulse as short as the 1840nm case does

When one puts together an 800nm, 22 fs FWHM pulse of $3 \times 10^{14} \text{ W/cm}^2$ and a 1840 nm, 64 fs FWHM pulse of $7.5 \times 10^{13} \text{ W/cm}^2$ (red square in Fig. 4(b)), one expect to observe an isolated single pulse of 180 attoseconds (after chirp management, 75 attoseconds).

One important results of this investigation is that an isolated single pulse of 230 attosecond pulse can be produced using a 33 fs FWHM pulse. When an 800 nm, 33 fs FWHM pulse of $5 \times 10^{14} \text{ W/cm}^2$ is mixed with an 1840 nm, 64 fs FWHM pulse of $2.9 \times 10^{13} \text{ W/cm}^2$ (black square in Fig. 4(a)), an isolated single pulse of 230 attoseconds is expected to be produced. This pulse can be even shortened to 170 attoseconds, below 200 attoseconds.

4. Summary

The effect of the mixing of pulsed two color fields on the generation of an isolated attosecond pulse has been systematically investigated in this work. One main color is 800 nm and the other color (or secondary color) is varied from 1.2 to 2.4 μm . The parameters chosen for the two color fields are those which are readily available in laboratories. This work shows that the continuum length behaves in a similar way to the behavior of the difference in the square of the amplitude of the strongest and next strongest cycle.

This continuum length behaves in a complicated manner, depending on the parameters of the pulsed two color fields. For given pulse widths of two color fields, a longer wavelength of the secondary field is more favorable to the longer continuum length than a shorter wavelength. When the mixing ratio of intensities is small at the level of 1% or less, the optimal wavelength for the longer continuum shifts toward shorter wavelength side, as the mixing ratio is increased. There is a certain mixing ratio of intensities at which the continuum length bifurcates, i.e., the existence of two optimal wavelengths. As the mixing ratio is further increased, each branch bifurcates again into two sub-branches. This 2D map analysis of the mixing ratio and the wavelength of the secondary field easily allows one to select a proper wavelength and the mixing ratio for a given pulse duration of the primary field. It is demonstrated that one can produce sub-100 attosecond pulse using an 11 fs FWHM 800 nm laser pulse with a proper mixing of an 1840 nm pulse. Furthermore the result shows that a 33 fs FWHM, 800 nm light pulse can produce an isolated pulse below 200 as, when properly mixed

Acknowledgment

The authors would like to acknowledge Dr. Zhinan Zeng for providing initial code for HHG simulation. This work has been supported in part by BK21 project funded by the Korea Research Foundation and in part by Basic Research Program (Grant No. KRF-2007-313-C00184) funded by Korean Science and Engineering Foundation KOSEF.